Published in final edited form as:
J Magn Reson Imaging. 2013 January ; 37(1): 243–248. doi:10.1002/jmri.23750.

Compressed-Sensing Multi-Spectral Imaging of the Post-Operative Spine

Pauline W. Worters, PhD[*,1], **Kyunghyun Sung, PhD**[1], **Kathryn J. Stevens, MD**[1], **Kevin M. Koch, PhD**[2], and **Brian A. Hargreaves, PhD**[1]

[1]Department of Radiology, Stanford University, Stanford, California

[2]Applied Science Laboratory, GE Healthcare, Waukesha, Wisconsin

Abstract

Purpose—To apply compressed sensing (CS) to *in vivo* multi-spectral imaging (MSI), which uses additional encoding to avoid MRI artifacts near metal, and demonstrate the feasibility of CS-MSI in post-operative spinal imaging.

Materials and Methods—Thirteen subjects referred for spinal MRI were examined using T2-weighted MSI. A CS undersampling factor was first determined using a structural similarity index as a metric for image quality. Next, these fully sampled datasets were retrospectively undersampled using a variable-density random sampling scheme and reconstructed using an iterative soft-thresholding method. The fully- and under-sampled images were compared by using a 5-point scale. Prospectively undersampled CS-MSI data were also acquired from two subjects to ensure that the prospective random sampling did not affect the image quality.

Results—A two-fold outer reduction factor was deemed feasible for the spinal datasets. CS-MSI images were shown to be equivalent or better than the original MSI images in all categories: nerve visualization: $p = 0.00018$; image artifact: $p = 0.00031$; image quality: $p = 0.0030$. No alteration of image quality and T2 contrast was observed from prospectively undersampled CS-MSI.

Conclusion—This study shows that the inherently sparse nature of MSI data allows modest undersampling followed by CS reconstruction with no loss of diagnostic quality.

Keywords

Metallic implants; Distortion correction; Susceptibility; Fast spin echo; Compressed sensing

INTRODUCTION

Compressed sensing (CS) has seen many recent developments, enabling its use in clinical MRI, since its first description in MRI by Lustig et al (1). An area that could lend itself particularly well to CS is MRI near metallic implants, where recently developed methods apply additional encoding to resolve and correct for metal-induced spatial distortion (2–4). These methods, generally known as multi-spectral imaging (MSI), have a relatively long acquisition time (at 5–10 minutes, despite acceleration strategies (5)) due to the extra encoding needed to resolve the large range of off-resonance frequencies induced by the presence of metal.

[*]Correspondence to: Pauline W. Worters, Lucas Center for MRI/S, 1201 Welch Road, Stanford, CA 94305-5488, Phone: (650) 721-6123, Fax: (650) 723-5795, worters@stanford.edu.

There are two recently developed MSI methods that have enabled distortion-free MRI in clinically feasible times. In slice encoding for metal artifact correction (SEMAC), 2D slices are excited and imaged with extra (3D) slice phase encoding (which is immune to off-resonance) to resolve the spatial slice distortion induced by extreme susceptibility effects (3). In multi-acquisition variable-resonance image combination (MAVRIC), a slightly different approach is used in which a volume is repeatedly excited with multiple overlapping frequency-selective excitations and scanned in 3D (2). Fundamentally, both of these methods seek to achieve the same goal of encoding frequency and spatial domains (i.e., *f*-*r* space). To perform this encoding, SEMAC uses spatial bins[1] and MAVRIC uses spectral (or frequency) bins. The more recent version MAVRIC-SL (a.k.a. VS-MSI, Hybrid) (4) combines the advantages of SEMAC and the original MAVRIC for a volume-selective, clinically feasible MSI acquisition. The extra phase encoding or repeated multi-frequency sampling is the primary reason for increased acquisition time.

Regardless of the particular MSI acquisition method used, it is vital to note that the total amount of signal (or information) is almost unchanged by the presence of metal; therefore the amount of signal within each bin is sparse. Typically in SEMAC and MAVRIC-SL, the signal near metal within each bin has a potato-chip-like appearance and most of the 3D image of each bin is composed of noise. The sparsity in MAVRIC is slightly different as the central/on-resonance bin is less sparse compared to the other off-resonance bins. Nonetheless, there is an inherent sparsity in MSI acquisitions that could be used to reduce acquisition time and perhaps improve image reconstruction quality. Lu presented work on reducing noise in SEMAC by using a singular value decomposition approach and taking advantage of redundancy between coils (6). Some other preliminary work applied CS to MSI acquisitions with a promising degree of success – Lu used a total variation minimization and POCS-based approach to CS (7, 8) while Koch applied parallel imaging and then CS reconstruction sequentially (9). These recent advances serve as a compelling motivation for this study.

In this work, we investigate the applicability of CS to post-operative spinal MSI with the goal of using this routinely in clinical practice. The number of lumbar spinal fusions is rapidly increasing in the United States, reaching 368,000 in 2007, and this number is projected to rise (10, 11). Furthermore, as many as 30% of patients remain symptomatic after surgery and require follow-up treatment including repeat surgery. Unfortunately, the metal hardware in these patients causes severe imaging artifacts on MRI and CT, and the imaging modalities currently available clinically often provide suboptimal assessment of these patients. MRI could potentially be excellent at depicting spine disease in patients with recurrent or residual symptoms after spinal surgery, and MSI could have a significant impact on clinical practice. However, the long imaging times of MSI currently limit its use in patients with severe back pain; furthermore, parallel imaging is difficult to apply in spine imaging due to incompatible coil array sensitivity variation. The imaging time reduction achieved by CS could facilitate MR imaging of patients in severe pain who are unable to withstand long acquisition times.

The goal of this work is to demonstrate CS-MSI in human subjects with spinal hardware. First, we demonstrated the feasibility of CS-MSI by retrospective application to a fully-sampled T2-weighted dataset from thirteen subjects. Second, we acquired prospectively undersampled CS-MSI to verify the consistency of T2-weighted contrast and image quality in MSI of the spine in two subjects.

[1]In MSI, a bin refers to one of multiple excited volumes that is spatially encoded in 3D and is later combined with other bins to form the final 3D distortion-free volumetric image.

MATERIALS AND METHODS

The retrospective studies were acquired using a 1.5 T MRI system (Signa HDx, GE Healthcare, Waukesha, WI) while the prospective studies were acquired using a 3.0 T MRI system (MR 750, GE Healthcare, Waukesha, WI). Informed consent was taken from all subjects according to our institution's IRB protocol.

Compressed Sensing Reconstruction

All reconstructions used an Intel Core2Duo machine (2.4 GHz, RAM 2 GB, bus speed 1.07 GHz, Mac OS X 10.6). A Gaussian-weighted variable-density random sampling pattern with the following parameters was used: probability function $\sum_{n=1}^{N} g(n) = \left\{ \exp\left(\frac{\alpha(n - N/2)}{2N} \right) \right\}^{0.75}$, where $\alpha = 3.0$. For each ky-kz point, a random number is generated and if the number is less than the probability function at ky, then the point is sampled, otherwise, the point is not sampled.

For the CS reconstruction, an approximate message passing (AMP) algorithm was used to enable short computational time (12). The AMP algorithm is a variation of an iterative soft-thresholding method (13) and Fig. 1 gives an overview of the AMP algorithm that performs the L1 minimization in the wavelet domain. A 2D wavelet transform (Daubechies 4, in y–z) was used and the iteration loop was performed for each bin, coil and readout location (after readout Fourier transform). The thresholding level is determined by multiplying a noise variance σ and an optimally tuned factor λ (14). The noise variance σ is computed by the median magnitude value of the highest wavelet sub-band at each iteration and the factor λ is set according to the undersampling factor as described in (14). The residual is calculated as the difference between the new and input data at sampled (not synthesized) k-space locations. The stopping criterion was met when the normalized difference of the root-mean-squared (i.e., L2-norm) of two successive residuals was less than 0.1%.

Homodyne processing for partial Fourier reconstruction was applied after the AMP step. Also, a surface coil intensity correction similar to the correction described in (15) was implemented to reduce the anterior-posterior signal intensity variation due to differing proximity from the linear spine array coil.

Retrospective Study

First, the reduction factor was determined using a structural similarity (SSIM) index, which is a reference-based quantitative measure (16). Due to the non-linear and noise-altering behavior of CS-type reconstructions, many conventional quantitative measures, such as root-mean-squared error, do not always accurately or realistically reflect the quality of non-linear reconstruction methods and as such, there remains no widely accepted measure for CS reconstructions. To the best of our knowledge, a fully quantitative assessment of CS-type reconstructions is an ongoing research area. The SSIM method normalizes the image luminance and contrast, and has been shown to be a very good indicator for the perceived image quality in image processing. Therefore, for this preliminary step of determining the reduction factor, SSIM was chosen to assess the CS image quality and to try to represent a user perception (as semi-quantitative radiologist scoring is used later for the main study). A full quantitative assessment of CS-type reconstruction is beyond the scope of this paper. An average SSIM greater than 0.95 (with 1.0 being best and −1.0 being worst) within a region-of-interest (ROI) located at the center of the spine was imposed to determine the reduction factor. Three outer reduction factors of 2.0, 2.5, and 3.0 (which refer to the undersampling compared to the fully-sampled data in the non-calibrating region) were tested on a single bin from a representative MSI acquisition. The calibration region was set to 24×24 in ky-kz.

Next, thirteen T2-weighted sagittal spine datasets acquired from patients with spinal hardware were undersampled with a reduction factor (as determined by the SSIM metric) and reconstructed using AMP. All spine acquisitions were made with a six- or eight-channel linear array receive-only coil. The MSI acquisition parameters were: 1.5 T; TE = 90–110 ms; TR = 4–6 s; matrix resolution = 256×224; FOV = 26–28 cm; slice thickness = 4 mm; echo train length = 18–20; RF bandwidth = 1.6 kHz; readout bandwidth = 977 Hz/pixel; half-Fourier (ky) acquisition with 24 phase-calibration lines; acquisition time 4–8 minutes.

The original and CS images were anonymized and compared side-by-side (randomized to left and right locations) by an experienced radiologist (14 years of musculoskeletal radiology) using a 5-point scale in three categories: (1) visualization of nerves and nerve roots; (2) image artifact (metal-induced and otherwise); and (3) overall image quality. A single-person evaluation was used here as this study was designed to be an initial, preliminary investigation to determine the feasibility of CS in spinal MSI. After de-blinding of images, the 5-point scale translates to: −2: CS much worse than original; −1: CS somewhat worse than original; 0: CS same as original; 1: CS somewhat better than original; 2: CS much better than original. A one-sided, paired Wilcoxon test was performed against the null hypothesis that CS images are somewhat worse than the original. If the null is rejected ($p < 0.05$), this indicates that the CS images are the same as or better than the original, within the tolerance of "somewhat worse" to "same as".

Prospective Acquisition

In this section, prospectively undersampled MSI acquisitions were performed in two subjects to verify that the view-ordering scheme used to achieve the random sampling pattern would not degrade the image quality in T2-weighted MSI. From each subject, a reference half-Fourier and a matching randomly-sampled half-Fourier acquisition were made with the following common parameters: 3 T, 6-channel linear receive coil, sagittal, TE = 120 ms; TR = 3.5 s; matrix resolution = 256×224; FOV = 26–28 cm; slice thickness = 4 mm; number of sections = 26–32; echo train length = 20; RF bandwidth = 2 kHz; readout bandwidth = 977 Hz/pixel; number of bins = 22; overlapping bins; half-Fourier acquisition; fast recovery (tip-up). Despite the theoretical challenge of using parallel imaging in spine imaging, an auto-calibrated parallel imaging (ARC (17)) reduction of 2× was used in the reference MSI to reduce the acquisition time to 9+ minutes, which is just about clinically feasible. The outer reduction factors used in the CS acquisitions were 2.6× and 3.0×, giving acquisition times of 7+ minutes. Again, the Gaussian-weighted random-sampling scheme was used to undersample the 3D data in ky-kz space, and the view-ordering of the randomly sampled k-space into echo-trains used a non-separable ky-kz method following that described in (18).

RESULTS

Figure 2 shows images reconstructed from a fully sampled data and at three undersampling factors with the corresponding structural similarity (SSIM) maps. The mean ± standard deviation and the range of SSIM values within a region-of-interest at the spinal canal are also shown in Fig. 2. With these results, in order to maintain a reasonable image quality (SSIM > 0.95), an outer undersampling factor of 2.0 was chosen for the retrospective study.

Figure 3 shows sagittal images from two subjects from the retrospective study. Statistical analysis of the radiologist scoring indicates that retrospective CS-MSI images are equivalent or better than the original MSI images, within the uncertainty of "somewhat worse" to "same as", for all categories: nerve visualization: $p = 0.00018$; image artifact: $p = 0.00031$; image quality: $p = 0.0030$. Multi-slice 2D fast spin echo (FSE) images acquired at high readout bandwidth (977 Hz/pixel) are also shown as a reference to illustrate the distortion correction

capability of the MSI technique. The percentage sampled shown combines the reduction due to ky-kz corner cutting, half-Fourier and with or without random undersampling. Overall, the retrospective undersampling applied here would translate to an approximate acquisition time reduction from about 4–8 minutes to 2–5 minutes.

Figure 4a plots the half-Fourier k-space acquired in the reference, regularly sampled acquisition and the CS randomly sampled acquisition. The colors refer to different echoes along the echo train. As T2-weighted data were acquired, the earlier echoes are acquired at the edge of ky and the later echoes towards the center of ky, as indicated by the arrows on the echo-train pathways (black lines). Note that the modulation of k-space due to relaxation is slightly different than for the regularly sampled case because a variable-density sampling scheme is used (i.e., more echoes are acquired in the central region in the randomly sampled scheme compared to the regularly sampled scheme). Figure 4b shows the sagittal images from 2D FSE, standard and CS MSI acquisitions in a subject at 3 T with metallic hardware. The MSI images were acquired with the k-space plots from Fig. 4a; the standard and CS MSI images demonstrate comparable image contrast and quality with slight blurring in the CS image. The solid arrows point to a neural foramen that is obscured in the 2D FSE image. The net percentage sampled k-space for this particular subject were 25% with ARC and 20% with CS, and the acquisition times were 10 min and 8:13 min, in the same order.

DISCUSSION

Multi-spectral imaging methods provide dramatic reduction of distortion in MR images of tissue near metallic implants. Recent studies have shown improved clinical care resulting from these methods (19, 20). However, in the case of post-operative spinal imaging, MSI methods sometimes have limited usage in patients with severe pain, who are unable to lie supine for the long period of time necessary for an MR examination without parallel imaging. With the use of compressed sensing in MSI, the acquisition times are significantly reduced, enabling this new technology to be used to improve patient care in these post-operative patients. Future studies may explore the use of CS to improve spatial resolution rather than to reduce scan times.

In the retrospective study, we have demonstrated the ability to undersample the data approximately two-fold while maintaining acceptable diagnostic image quality. The results from the retrospective study appears to be applicable to prospective CS-MSI where reductions greater than two-fold were achieved by optimizing the acquisition parameters, such as increasing the encoding size of each bin and using heavily overlapping bins. No parallel imaging was used in the retrospective 1.5 T spine imaging due to the incompatibility of the coil sensitivity variation and prescription geometry. However, due to patient comfort reasons, parallel imaging had to be used for the reference 3 T MSI acquisition otherwise the acquisition time would be prohibitively long. With other clinical applications such as knee and hip MSI, reconstruction methods that perform parallel imaging and CS reconstructions, such as L1-SPIRiT (21), could be used to further increase reduction factors and also potentially reduce reconstruction times compared to sequential applications of parallel imaging and CS reconstructions (9).

A relatively simple variation of the iterative soft-thresholding method was used to reconstruct the undersampled data. The AMP algorithm is data driven and calibrates the soft-thresholding level depending on the data signal level and enables short computational time by correcting the residual bias from the previous iteration (12). The input parameters were not adjusted per subject for reconstruction – the same parameters were used for all cases and we did not observe any failures of the reconstruction algorithm. However, typical reconstruction times are lengthy (on average taking slightly less than one hour), which is

currently limiting its integration into routine clinical applications. Admittedly, there are multi-core, hyper-threaded machines that could be used to speed up the reconstruction time by about five to ten times. Apart from using better equipped computers, there are other ways of potentially reducing the reconstruction times. Currently, the AMP algorithm is applied per bin and per coil; therefore, methods that reduce the number of bins and coils would proportionately reduce the reconstruction time. Such methods include coil compression and virtual coil synthesis (22, 23), which reduce the number of coils in k-space while preserving coil sensitivity and/or phase information. We have used a sum-of-squares combination of multiple bins that is typically applied at the final reconstruction stage, but other strategies of pre-FFT bin combination, such as a simple complex sum (5), could also allow a significant reduction in the CS processing. With the latter approaches, methods to deal with phase variations and noise must be used to maintain similar image SNR to that of the sum-of-squares approach.

There has been some preliminary work that has applied random sampling to 3D FSE acquisitions. (7–9). Unlike in single-echo or steady-state sequences, the spin echo train and view-ordering scheme in 3D FSE is important and affects the image contrast, blurring and appearance of artifacts. Although only half-Fourier acquisitions were used here to reduce acquisition time, the view-ordering method used is equally applicable to full-Fourier and radial/centric encoding schemes. In a few cases in the retrospective study, the CS images looked slightly blurrier compared to the original images, which may be due to the de-noising effect of the CS reconstruction, similar to Lu's work in (6), as noise can make an image appear sharper. In the prospective study, we made a straightforward application of the non-separable view-ordering scheme that was used in the regularly sampled acquisition to the randomly sampled acquisition. Although minimal blurring was apparent on some of the images, no significant detrimental effects were observed in the CS images. The blurring could be somewhat anticipated, as a higher proportion of the echoes were acquired in the central k-space region in the CS case compared to the regular case (Fig. 4a) – this leads to more relaxation-induced modulation of k-space close to the center, hence more blurring. Strategies such as variable refocusing RF flip angles and shorter echo trains could be used to mitigate the blurring. A proper analysis of the spatial resolution effects from k-space modulation and/or CS reconstructions are beyond the scope of this paper.

In conclusion, we have demonstrated that CS can be applied in MSI data with modest (2–3×) additional undersampling factors without degrading image quality. While we anticipate that greater reduction factors will be made possible by improved reconstruction techniques and the inclusion of parallel imaging, this initial study is significant in demonstrating the feasibility of reduced acquisition times in spine MSI examinations.

Acknowledgments

The authors would like to thank Marcus T. Alley and Mark J. Murphy for advice on code implementation, Michael Lustig, John M. Pauly and Tao Zhang for helpful discussion on reconstruction, and Jarrett K. Rosenberg for statistical advice.

Grant Sponsors: This work was supported by NIH R21-EB008190, the Richard M. Lucas Foundation and General Electric Healthcare.

REFERENCES

1. Lustig M, Donoho D, Pauly JM. Sparse MRI: The application of compressed sensing for rapid MR imaging. Magn Reson Med. 2007; 58:1182–1195. [PubMed: 17969013]

2. Koch KM, Lorbiecki JE, Hinks RS, King KF. A multispectral three-dimensional acquisition technique for imaging near metal implants. Magn Reson Med. 2009; 61:381–390. [PubMed: 19165901]

3. Lu W, Pauly KB, Gold GE, Pauly JM, Hargreaves BA. SEMAC: Slice Encoding for Metal Artifact Correction in MRI. Magn Reson Med. 2009; 62:66–76. [PubMed: 19267347]

4. Koch KM, Brau AC, Chen W, Gold GE, Hargreaves BA, Koff M, McKinnon GC, Potter HG, King KF. Imaging near metal with a MAVRIC-SEMAC hybrid. Magn Reson Med. 2011; 65:71–82. [PubMed: 20981709]

5. Hargreaves BA, Chen W, Lu W, Alley MT, Gold GE, Brau ACS, Pauly JM, Pauly KB. Accelerated slice encoding for metal artifact correction. J Magn Reson Imaging. 2010; 31:987–996. [PubMed: 20373445]

6. Lu W, Pauly KB, Gold GE, Pauly JM, Hargreaves BA. Slice encoding for metal artifact correction with noise reduction. Magn Reson Med. 2011; 65:1352–1357. [PubMed: 21287596]

7. Lu, W.; Pauly, KB.; Gold, GE.; Pauly, JM.; Hargreaves, BA. Proc Intl Soc Magn Reson Med. Stockholm: 2010. Compressive Slice Encoding for Metal Artifact Correction; p. 3079

8. Lu, W.; Deng, J.; Lu, Y.; Gold, GE.; Hargreaves, BA. Proc Intl Soc Magn Reson Med. Montreal: 2011. POCS-based Compressive Slice Encoding for Metal Artifact Correction.

9. Koch, KM.; Koff, MA.; Potter, HG. Proc Intl Soc Magn Reson Med. Montreal: 2011. Combined Parallel Imaging & Compressed Sensing on 3D Multi-Spectral Imaging Near Metal Implants; p. 3172

10. Abraham DJ, Herkowitz HN, Katz JN. Indications for thoracic and lumbar spine fusion and trends in use. Orthop Clin North Am. 1998; 29:803. [PubMed: 9756973]

11. Elixhauser A, Andrews RM. Profile of inpatient operating room procedures in US hospitals in 2007. Arch Surg. 2010; 145:1201–1208. [PubMed: 21173295]

12. Donoho DL, Maleki A, Montanari A. Message-passing algorithms for compressed sensing. Proc Natl Acad Sci USA. 2009; 106:18914–18919. [PubMed: 19858495]

13. Daubechies I, Defrise M, DeMol C. An iterative thresholding algorithm for linear inverse problems with a sparsity constraint. Commun Pure Appl Math. 2004; 57:1413–1457.

14. Maleki A, Donoho D. Optimally tuned iterative reconstruction algorithms for compressed sensing. IEEE J Sel Topics Signal Process. 2010; 4:330–341.

15. Murakami JW, Hayes CE, Weinberger E. Intensity correction of phased-array surface coil images. Magn Reson Med. 1996; 35:585–590. [PubMed: 8992210]

16. Wang Z, Bovik AC, Sheikh HR, Simoncelli EP. Image quality assessment: from error visibility to structural similarity. IEEE Trans Image Process. 2004; 13:600–612. [PubMed: 15376593]

17. Brau ACS, Beatty PJ, Skare S, Bammer R. Comparison of reconstruction accuracy and efficiency among autocalibrating data-driven parallel imaging methods. Magn Reson Med. 2008; 59:382–395. [PubMed: 18228603]

18. Busse RF, Brau AC, Vu A, Michelich CR, Bayram E, Kijowski R, Reeder SB, Rowley HA. Effects of refocusing flip angle modulation and view ordering in 3D fast spin echo. Magn Reson Med. 2008; 60:640–649. [PubMed: 18727082]

19. Chen CA, Chen W, Goodman SB, Hargreaves BA, Koch KM, Lu W, Brau AC, Draper CE, Delp SL, Gold GE. New MR imaging methods for metallic implants in the knee: artifact correction and clinical impact. J Magn Reson Imaging. 2011; 33:1121–1127. [PubMed: 21509870]

20. Hayter CL, Koff MF, Shah P, Koch KM, Miller TT, Potter HG. MRI After Arthroplasty: Comparison of MAVRIC and Conventional Fast Spin-Echo Techniques. Am J Roentgenol. 2011; 197:W405–W411. [PubMed: 21862766]

21. Lustig M, Pauly JM. SPIRiT: Iterative self-consistent parallel imaging reconstruction from arbitrary k-space. Magn Reson Med. 2010; 64:457–471. [PubMed: 20665790]

22. Zhang, T.; Lustig, M.; Vasanawala, SS.; Pauly, JM. Proc Intl Soc Magn Reson Med. Montreal: 2011. Array Compression for 3D Cartesian Sampling; p. 2857

23. Beatty, PJ.; Sun, W.; Brau, ACS. Proc Intl Soc Magn Reson Med. Toronto: 2008. Direct Virtual Coil (DVC) Reconstruction for Data-Driven Parallel Imaging; p. 8

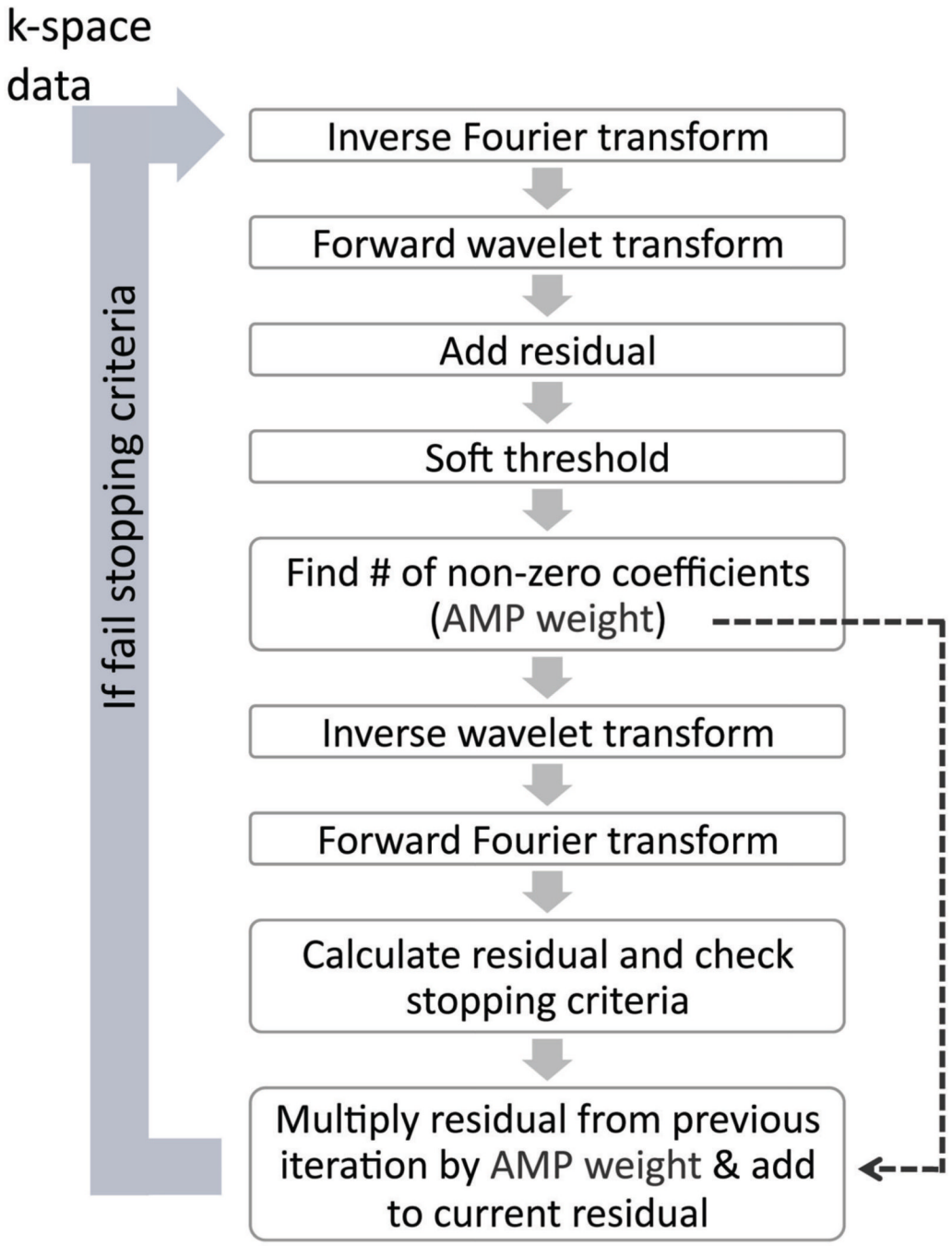

Figure 1.

Approximate Message Passing (AMP), a variant of iterative soft thresholding, is used in the CS reconstruction. The 2D Fourier transform (in y ▫ z) and Daubechies 4 wavelet transform were used. The soft-thresholding step is data-driven and based on the undersampling factor and signal level in the highest wavelet sub-band. The AMP term (previous iteration's residual multiplied by AMP weight) enables fast computation. The stopping criterion is met when the normalized difference of the L2-norm of successive residuals is less than 0.1%.

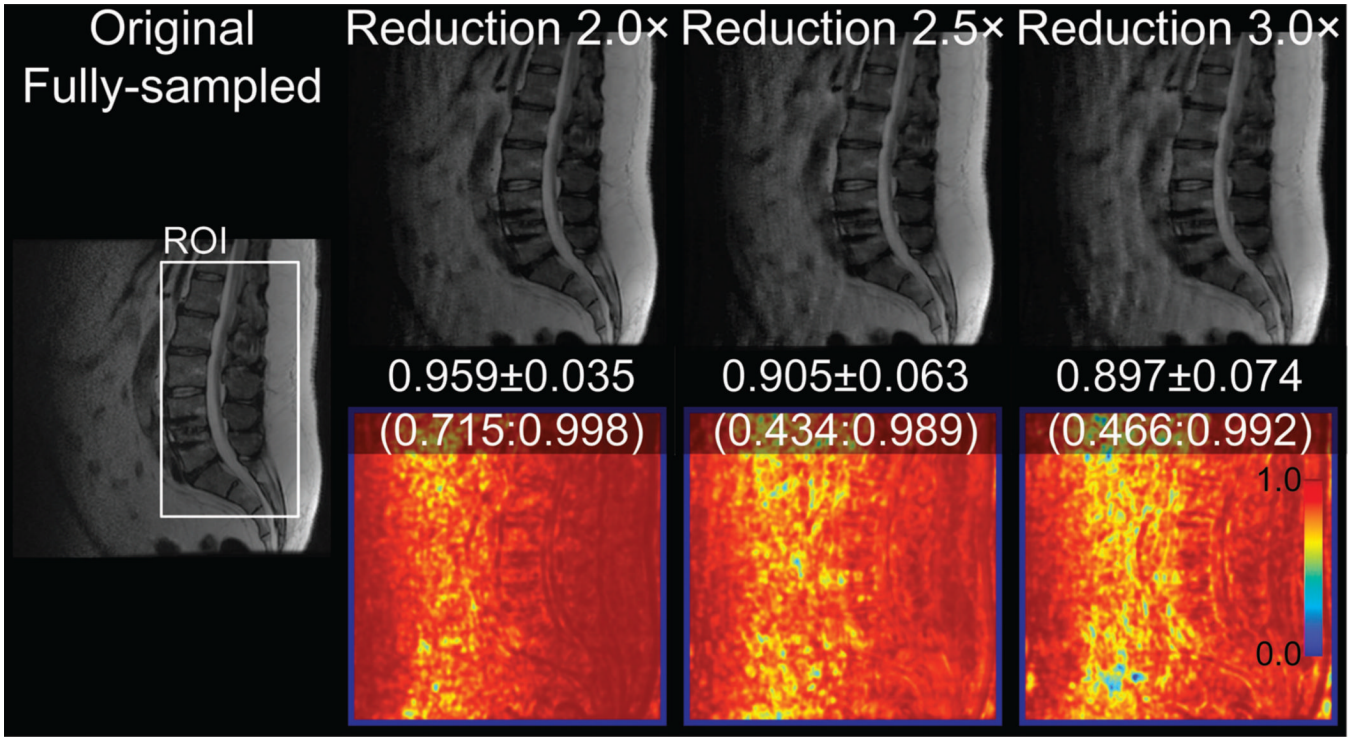

Figure 2.
Sagittal spine images of the fully-sampled half-Fourier and reconstructed at 2–3× outer reduction factors, with SSIM maps (bottom) obtained by comparison to the fully-sampled image. The values refer to the SSIM average ± standard deviation (minimum:maximum) in the ROI.

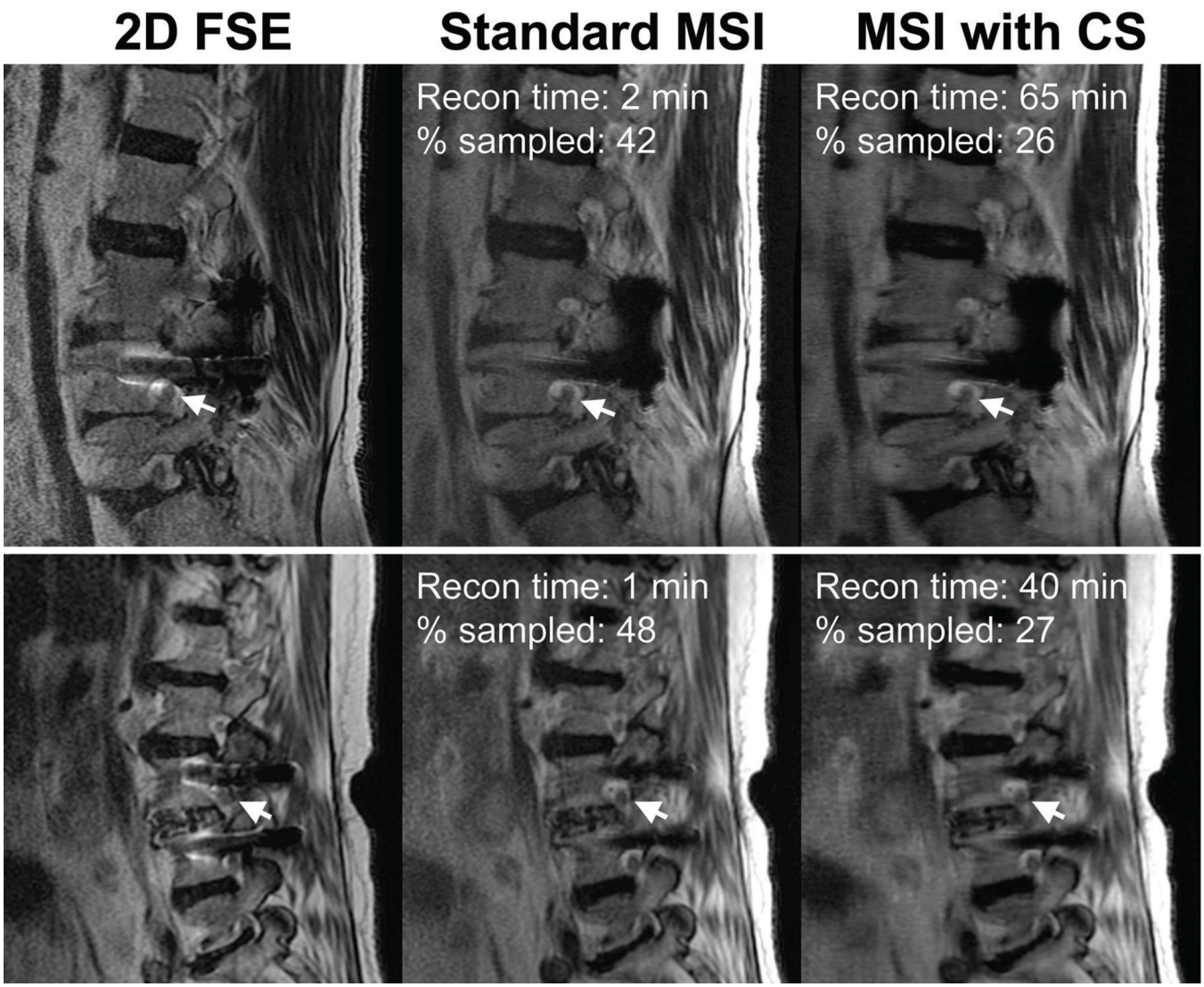

Figure 3.
Sagittal T2-weighted FSE and MSI slices from two subjects (top and bottom row) acquired at 1.5 T demonstrating the retrospective application of compressed sensing. 2D FSE images are shown to show the distortion induced by the presence of metal. The arrows point to nerves and neural foramina that are clearly depicted in the images acquired with MSI. The percentage sampled in the fully-sampled half-Fourier image is under 50% as corners in ky-kz space were not acquired.

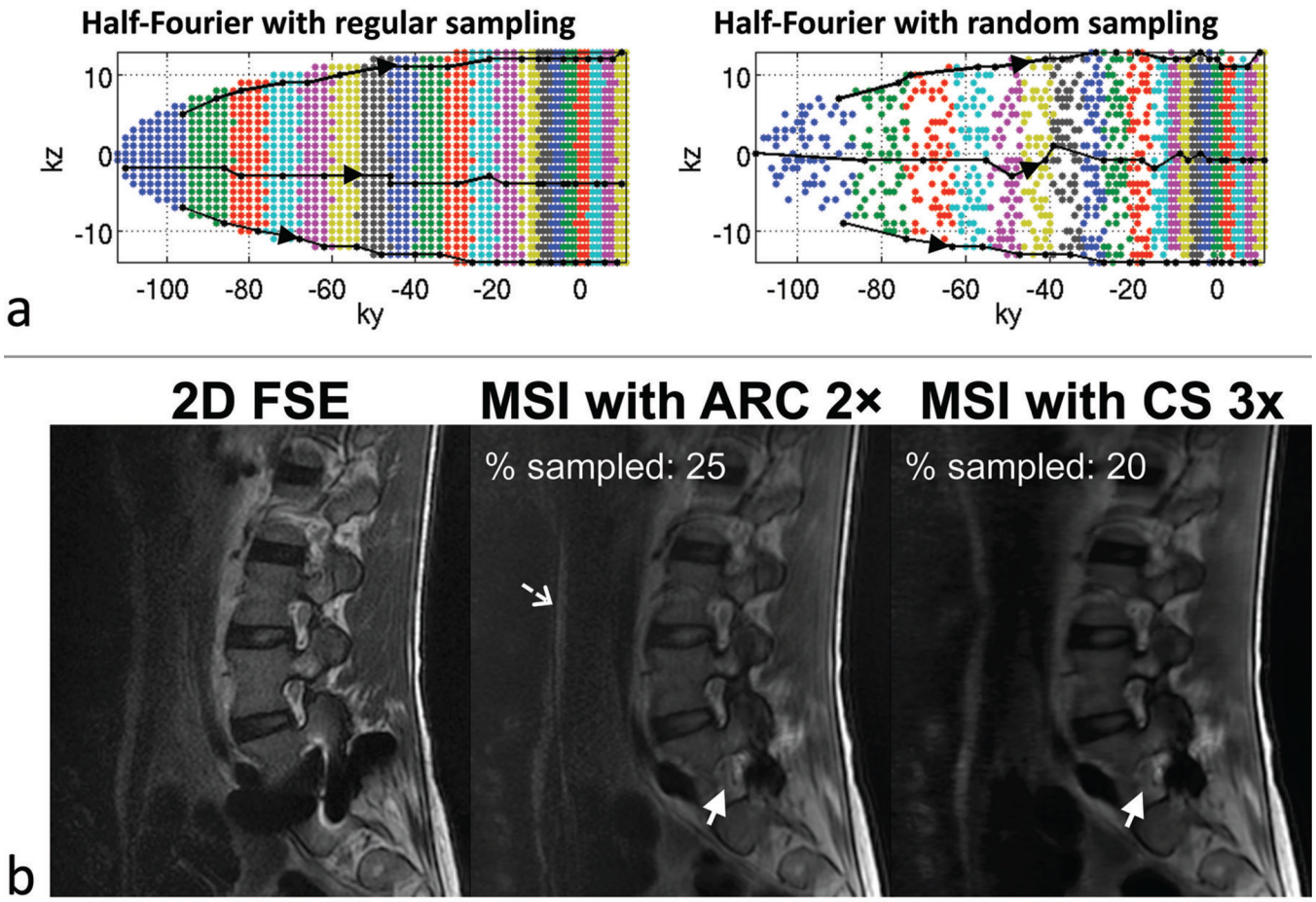

Figure 4.

(a) Acquired k-space plots in the reference regularly sampled acquisition and the CS randomly sampled acquisition with reduction factors of 2 and 3 respectively. The k-space plots correspond to the MSI images in (b). The colors refer to the echo numbers along the echo train (echo-train length = 20). Three example echo-train pathways (black lines) are shown in each k-space. (b) Sagittal T2-weighted acquisitions at 3 T with 2D fast spin echo (FSE), reference MSI with 2× parallel imaging in the anterior-posterior direction (acquisition time = 10 min) and CS-MSI with 3× outer reduction (acquisition time = 8:13 min). The solid arrows point to a neural foramen that is obscured on the 2D FSE image due to severe signal distortion. A slight parallel imaging artifact was seen (dashed arrow) due to the use of a linear coil array with sensitivity variation largely in the superior-inferior direction. Despite the slight blurring in the CS image, the overall image quality and contrast between both MSI acquisitions are comparable.